SCIENCE CHINA
Earth Sciences

• RESEARCH PAPER •

April 2014 Vol.57 No.4: 693–702
doi: 10.1007/s11430-013-4743-x

The effects of vertical viscosity coefficients with different distribution characteristics on classical Ekman spiral structure

MA HongYu[1,2,3], QIAO FangLi[2,3*] & DAI DeJun[2,3]

[1] *College of Physical and Environmental Oceanography, Ocean University of China, Qingdao 266100, China;*
[2] *First Institute of Oceanography, State Oceanic Administration, Qingdao 266061, China;*
[3] *Key Lab of Marine Science and Numerical Modeling, State Oceanic Administration, Qingdao 266061, China*

Received April 17, 2013; accepted August 19, 2013; published online January 3, 2014

The classical Ekman theory tells us that the ocean surface current turns to the right (left) side of wind direction with 45° in the north (south) hemisphere, but the observation and research results show that the surface current deflexion angle is smaller than 45° in the Arctic and high latitude areas while larger than 45° in the low latitude areas. In order to explain these phenomena, a series of idealized numerical experiments are designed to investigate the influence of vertical viscosity coefficients with different vertical distribution characteristics on the classical and steady Ekman spiral structure. Results show that when the vertical viscosity coefficient decreases with water depth, the surface current deflexion angle is larger than 45°, whereas the angle is smaller than 45° when the vertical viscosity coefficient increases with water depth. So the different observed surface current deflexion angles in low latitude sea areas and the Arctic regions should be attributed to the different vertical distribution characteristics of vertical viscosity coefficients in the upper ocean. The flatness of the Ekman spiral is not equal to one and does not show regular behaviors for the numerical experiments with different distribution of vertical viscosity. However, the magnitudes and directions of volume transport of Ekman spirals are almost the same as the results of classical Ekman theory, i.e., vertical viscosity coefficient distributions have no effect on the magnitudes and directions of volume transport.

Ekman spiral structure, vertical viscosity coefficient distribution, surface current deflexion angle, numerical experiment

Citation: Ma H Y, Qiao F L, Dai D J. 2014. The effects of vertical viscosity coefficients with different distribution characteristics on classical Ekman spiral structure. Science China: Earth Sciences, 57: 693−702, doi: 10.1007/s11430-013-4743-x

In the Arctic Ocean, Nansen discovered that the sea ice drifts to the right side of wind direction with an angle of 20° to 40°. Based on the observation, Ekman (1905) got the analytical solution, namely the classical Ekman drift currents theory by assuming that homogenous and steady wind flows over the infinitely broad ocean surface and the vertical viscosity coefficient in the ocean is constant. From the theory, we know that the angle between surface current direction and wind direction is 45° and turns to the right side of wind direction in the northern hemisphere. The current velocity decreases exponentially and the deflexion angle increases with depth, and then the Ekman spiral is formed. The Ekman spiral is a classical concept in physical oceanography. The Ekman theory reveals the movement state of sea water under the effect of steady, homogenous and lasting wind, the water depth influenced by wind, and the volume transport induced by wind. It is useful to explain the ocean processes such as convergence and divergence in the ocean and upwelling in coastal seas.

The classical Ekman theory shows that the deflexion angle of surface current should be 45° while the observations and studies show that the deflexion angle is different from

*Corresponding author (email: qiaofl@fio.org.cn)

the theory value in the ocean, i.e., it can be larger than 45° or smaller than 45°. Thorndike et al. (1982) pointed out that the angle between drifting direction of floating ice and geostrophic wind in the Arctic Ocean is 5° in autumn, winter and spring and 8° in summer. Considering the relationship between geostrophic wind and sea surface wind, Overland (1994) estimated that the angle is 33° in winter and 23° in summer. Based on the observations in the Arctic in 2010, Shu et al. (2012) found that the angle is about 40°. Kimura et al. (2000) pointed out that the angle between drifting direction of floating ice and geostrophic wind is 8.7° based on data from Okhotsk. Fukamachi et al. (2011) showed that the angle is 9.1°. Considering the angle between geostrophic wind and sea surface wind, we can conclude that the observed angles between sea surface current drifting direction and sea surface wind in high-latitude area were smaller than 45°. In the low-latitude ocean, the observations of R/P buoy near surface current deflexion angle relative to sea surface wind was 60°, larger than 45° (Price et al., 1986). In the data used by Price et al. (1986), the shallowest current was measured at water depth of 2 m from the sea surface. Later based on the LOTUS (Long Term Upper Ocean Study) data, Price et al. (1987) pointed out that the surface current deflexion angle is 80° with the uppermost current measured at 5 m away from the surface. So the observed deflexion angle by Price et al. (1987) is only an approximation, not the real surface current deflexion angle. From the observations and studies, one can find that the angle between the sea surface current drifting direction and sea surface wind usually is smaller than 45° in high latitudes and larger than 45° in the low latitude oceans.

The Ekman drift currents theory was achieved under the assumption that steady and homogenous wind acts on infinitely broad sea surface. Therefore, in the real ocean, finite water depth, unsteady wind and non-homogenous wind should have influence on Ekman spiral structure. So the angle between sea surface current drifting direction and sea surface wind should depart from 45°. On the other hand, the vertical viscosity coefficient was assumed to be constant in the classical Ekman drift currents theory. However, it is impossible that the vertical viscosity is uniform in the whole water depth in the real ocean. So it is meaningful to investigate the influence of vertical viscosity coefficients with different vertical distribution on Ekman spiral structure. Thomas (1975) chose an idealized vertical viscosity coefficient $v_E(z) = \kappa u_*(h-z)$, which decreases with depth linearly and got analytical solutions of Ekman spiral by using Bessel function, where $u_* = v_0/\kappa h$ is friction velocity, v_0 is the largest value of vertical viscosity coefficient at the sea surface, $\kappa \approx 0.4$, h is water depth, and z is positive downward. He pointed out that the sea surface current deflexion angle can be larger or smaller than 45°, which depends on the ratio of water depth and friction depth of Ekman spiral. Supposing the vertical viscosity coefficient $v_E(z) = \kappa u_* z$ (shearing velocity $u_* = (|\tau_s|/\rho)^{1/2}$) increasing linearly with depth, Madsen (1977) got analytical solutions of Ekman spiral in the ocean with infinite depth. In that case, the sea surface current deflexion angle is about 10°, much smaller than the result of classical Ekman theory. In the finite depth water, considering three kinds of vertical viscosity coefficients: constant value, exponential form $v_E(z) = v_0 e^{az}$, and power function form $v_E(z) = v_0(1+z/\alpha)^{\mu}$, Jordan et al. (1980) got analytical solutions with eigenfunction expandedness method, where v_0, a, α and μ are constants, z is positive upward. And their results suggested that the sea surface current deflexion angle is larger than 45° mostly when the vertical viscosity coefficients decrease with water depth (Jordan et al., 1980), the angle is smaller than 45° mostly when the vertical viscosity coefficients increase with water depth (Jordan et al., 1980). Huang (2009) studied the influence of anisotropy of vertical viscosity on the sea surface current deflexion angle and found that the deflexion angle can be larger than 45° or smaller than 45°, which depends on different vertical viscosity coefficients in *u* and *v* directions. From above, we can see that the influence of vertical viscosity coefficients on the structure of Ekman spiral had been investigated by previous studies. However, only idealized cases or the viscosity coefficients varying with water depth monotonically were considered. Moreover, they are lack of support from real physical processes to the idealized distribution of vertical viscosity, so it remains difficult to explain why the angle between sea surface current drifting direction and surface wind is usually smaller than 45° in high latitudes and larger than 45° in low latitudes.

Given the complex vertical distribution of viscosity coefficients in the real ocean, four categories of vertical viscosity coefficients were selected in this paper to investigate the influence of vertical viscosity coefficients on Ekman spiral structure by using numerical method.

1 Governing equations and discretization method

Assuming homogeneous ocean with infinitely depth, steady and homogenous wind acts on the sea surface. When friction force is equal to Coriolis force, the steady current is formed. The governing equations can be written as

$$-fv = \frac{\partial}{\partial z}\left(v_E \frac{\partial u}{\partial z}\right), \tag{1}$$

$$fu = \frac{\partial}{\partial z}\left(v_E \frac{\partial v}{\partial z}\right), \tag{2}$$

with the surface and bottom boundary conditions

$$z = 0: \qquad \rho_0 \nu_E \frac{\partial u}{\partial z} = \tau^x, \quad \rho_0 \nu_E \frac{\partial v}{\partial z} = \tau^y, \tag{3}$$

$$z \to \infty: \qquad u = 0, \quad v = 0, \tag{4}$$

where u and v are horizontal velocity, z is the vertical coordinates and positive downward, f is the Coriolis parameter, ν_E is vertical viscosity coefficient, density of sea water ρ_0 is constant, τ^x and τ^y are wind stresses in x and y directions respectively.

When the vertical viscosity coefficient is constant, one can easily get the analytical solutions of eqs. (1) and (2), which is the classical Ekman theory. But, it is difficult to get the analytical solutions when ν_E is not constant. In this paper, the governing eqs. (1) and (2) are discretized with central difference method and the numerical method is used to get the solutions of Ekman spiral structure.

In order to improve the computational accuracy of near-surface current velocity, we divide the whole depth into different layers and the layers in the near-surface are dense. Using second-order central difference method, the difference equations of the governing equations are

$$\begin{aligned} -fv(n) = {} & \left[\nu_E(n) + \nu_E(n-1)\right] \cdot \\ & \frac{u(n-1) - u(n)}{\left[z(n+1) - z(n-1)\right]\left[z(n) - z(n-1)\right]} \\ & - \left[\nu_E(n+1) + \nu_E(n)\right] \cdot \\ & \frac{u(n) - u(n+1)}{\left[z(n+1) - z(n-1)\right]\left[z(n+1) - z(n)\right]}, \end{aligned} \tag{5}$$

$$\begin{aligned} fu(n) = {} & \left[\nu_E(n) + \nu_E(n-1)\right] \cdot \\ & \frac{v(n-1) - v(n)}{\left[z(n+1) - z(n-1)\right]\left[z(n) - z(n-1)\right]} \\ & - \left[\nu_E(n+1) + \nu_E(n)\right] \cdot \\ & \frac{v(n) - v(n+1)}{\left[z(n+1) - z(n-1)\right]\left[z(n+1) - z(n)\right]}. \end{aligned} \tag{6}$$

The equations of boundary conditions are discretized by using one-order Euler difference scheme. From the difference equations of the governing equations and boundary conditions, one can get the systems of the linear equations of velocity u and v. And then the value of velocity can be obtained by solving the systems of the linear equations numerically.

In this study, the water depth is chosen as 120 m, water density is 1025 kg m^{-3}, Coriolis parameter is 1.453×10^{-4}, wind stress $\tau^x = 0$ N m^{-2}, $\tau^y = 0.1$ N m^{-2}.

2 Numerical experiments

Generally, the vertical distributions of vertical viscosity coefficients are determined by the physical processes in ocean. In order to study the influence of vertical viscosity coefficients with different distributions on the Ekman spiral structure, four categories of vertical viscosity coefficients are summarized and idealized to represent the actual vertical distributions of viscosity in different areas or dynamical environments. For the open oceans, the physical processes occurring at the air-sea interface, such as wind, surface waves and Langmuir circulation and so on, provide much mechanical energy to the turbulence in the upper ocean directly or indirectly. So the typical distribution characteristic is that the vertical viscosity coefficient decreases with water depth in the upper ocean (Huang et al., 2012). In the Arctic Ocean and high latitudes, because the ocean is covered by floating ice, the turbulence induced by air-sea interface processes, such as surface waves, is very weak. Thus the vertical viscosity coefficient increases first with water depth, and then decreases since mixing length will increase with depth. In coastal oceans, the vertical viscosity coefficient decreases with depth first because the effect of surface waves is becoming weak, and then increases because of the effect of tidal current at the bottom of sea (Yuan et al., 1993). In the shallow sea, if the effect of surface waves is very weak, the vertical viscosity coefficient will increase with water depth. In this paper, though considering these four cases (Table 1), we discuss the influence of the vertical distribution characteristics of the vertical viscosity coefficients on Ekman spiral structure. It is worth noting that the water depth (120 m) in numerical scheme is always larger than the Ekman depth (D_0 and D, which will be defined later) for the four cases, which means that the Ekman spiral we get by using numerical method is not influenced by the bottom boundary.

2.1 Vertical viscosity coefficient monotonically decreasing with water depth

In this case, three kinds of vertical viscosity coefficients with different attenuation styles and speeds (Figure 1, Table 1) are chosen, which are the exponential distribution like $\nu_E(z) = 0.01 + 0.1\mathrm{e}^{-z/5}$ with fast attenuation speed, the linear distribution $\nu_E(z) = 0.06 - 0.0005z$, and the exponential distribution like $\nu_E(z) = 0.1 - 0.1\mathrm{e}^{-\frac{\pi}{300}(h-z)}$ with slow attenuation speed.

For the first case, the vertical viscosity coefficient is chosen as $\nu_E(z) = 0.01 + 0.1\mathrm{e}^{-z/5}$, which decreases exponentially. The viscosity value is about 0.11 m^2 s^{-1} at the sea surface and 0.01 m^2 s^{-1} at about 20 m water depth. In order to indicate the depth where Ekman spiral structure can in-

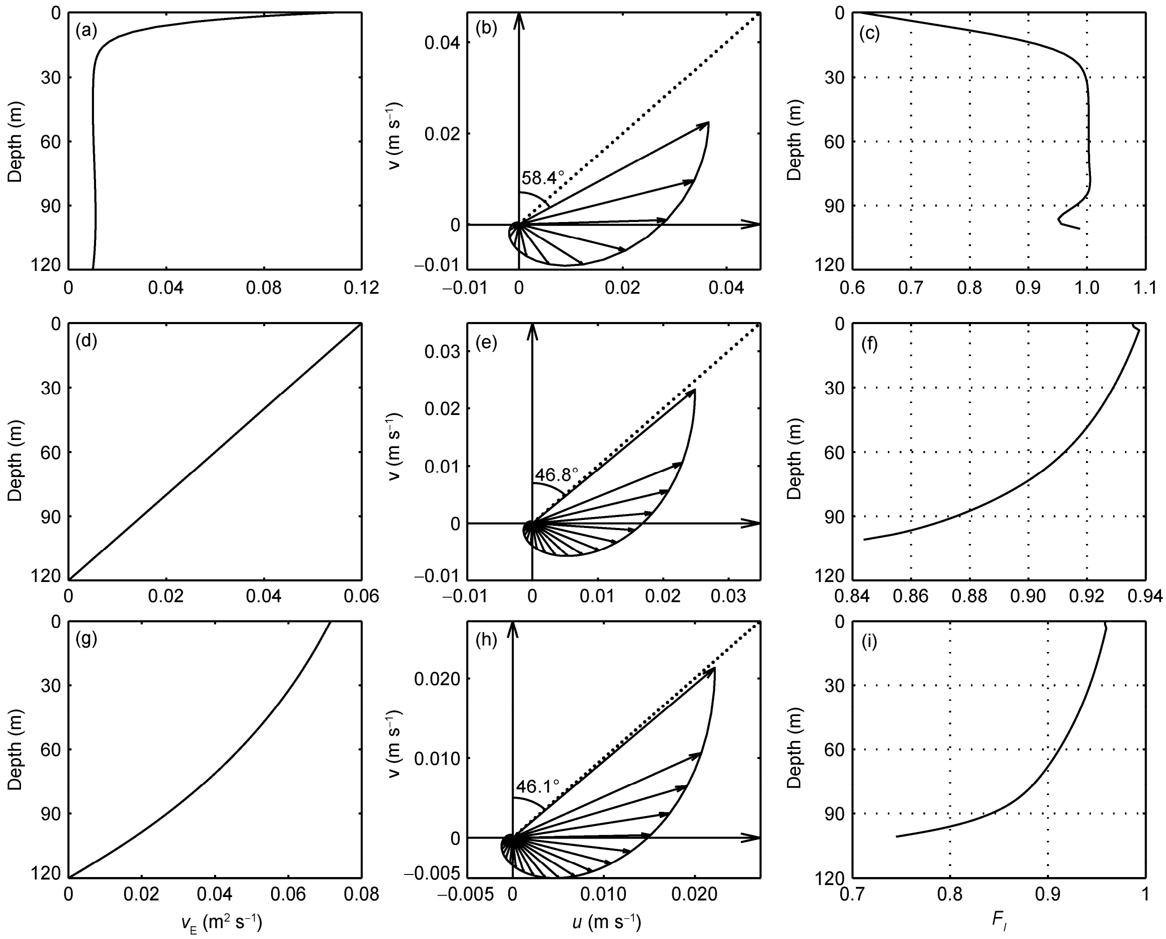

Figure 1 Three kinds of vertical viscosity coefficients ((a), (d) and (g)), the corresponding Ekman spiral structures ((b), (e) and (h), with dot lines indicating the 45° deflexion angle) and flatness F_l ((c), (f) and (i)).

Table 1 Vertical viscosity coefficients and the numerical results of surface current deflexion angle, volume transport, D_0 and D

Vertical viscosity coefficients v_E		Deflexion angle	Volume transport		D_0	D
			Magnitude	Direction		
Decreasing	$0.01+0.1e^{-z/5}$	58.4°	0.673	89.9°	47.6	55.8
	$0.06-0.0005z$	46.8°	0.672	89.9°	77.0	75.5
	$0.1-0.1e^{-\frac{\pi}{300}(h-z)}$	46.1°	0.672	89.9°	88.4	86.0
Increasing	$0.100001-0.1e^{-z/20}$	14.7°	0.710	91.4°	47.6	93.3
	$0.02+0.0005z$	42.4°	0.672	91.1°	61.2	70.5
	$0.02+0.1e^{-\frac{\pi}{150}(h-z)}$	44.0°	0.675	91.4°	65.7	72.6
Increasing and then decreasing		32.4°	0.673	89.8°	52.1	63.6
Decreasing and then increasing		54.8°	0.676	91.4°	72.5	82.4

fluence and compare with the result of classical Ekman theory, depths D_0 and D are defined. D_0 is defined as the depth where the velocity is equal to $e^{-\pi}$ of the velocity at sea surface, which is the same as the definition of the Ekman depth of the classical Ekman theory. In the layers from surface to D_0, one can get the mean value of vertical viscosity coefficient, $\overline{v_E}=\frac{1}{D_0}\sum_{z(1)=0}^{z(m)=D_0} v_E\left(z(i)\right)\mathrm{d}z(i)$, and then define the depth D as $\pi\sqrt{\frac{\overline{v_E}}{f/2}}$. The depth D is equal to the depth where classical Ekman drifting current can influence when the vertical viscosity coefficient is constant, $\overline{v_E}$. For the first case, $D_0=47.6$ m, $D=55.8$ m, they are all smaller than the water depth 120 m, which we have set in numerical scheme. Thus, we can believe that the Ekman spiral structure is not affected by the bottom boundary.

Meanwhile, depth D_0 is smaller than depth D, which means that the attenuation speed of Ekman drifting current in the vertical direction is faster than that with the constant vertical viscosity coefficient of $\overline{v_E}$. The Ekman spiral structure is shown in Figure 1(b), which represents the projection of currents at different depth from the sea surface to the bottom. Its surface current deflexion angle is 58.4°, larger than 45°. The flatness of Ekman spiral is computed from the function $F_l = \frac{\partial S}{\partial z}\left(S\frac{\partial \theta}{\partial z}\right)^{-1}$ given by Price et al. (1999), where S represents the magnitude of current, θ is the deflexion angle. The flatness of Ekman spiral is a ratio of the speed of current velocity attenuating and the speed of current direction turning. Generally, $F_l < 1$ means that the speed of current direction turning is faster than the speed of current velocity attenuation. On the contrary, $F_l > 1$ means that the speed of current direction turning is slower than the speed of current velocity attenuation. For the classical and steady Ekman drift current in deep water, the flatness F_l is equal to 1. From Figure 1(c), we can see that F_l increases fast when the vertical viscosity coefficient decreases with water depth in 0–30 m layer. Below the depth of 30 m, vertical viscosity coefficient almost does not change with water depth, so the flatness F_l is almost equal to 1. The flatness F_l is smaller than one in water depth of 0–30 m, which implies that the speed of current direction turning is larger than the speed of current velocity attenuation. It must be noted that the Ekman drift current velocity is very small in water depth below 100 m and the computation error of spiral flatness may be large. So only the flatness F_l above 100 m is shown in Figure 1(c).

For the second case, the vertical viscosity coefficient $v_E(z) = 0.06 - 0.0005z$ decreases with water depth linearly (Figure 1(d)). Its value is 0.06 $m^2\ s^{-1}$ at the sea surface, zero at the sea bottom (z=120 m). In this case, $D_0 = 77.0$ m, $D = 75.5$ m, and they are almost the same. The surface current deflexion angle is 46.8° (Figure 1(e)). The flatness F_l is smaller than one (Figure 1(f)), i.e., the speed of current direction turning is larger than the speed of current velocity decreasing. Moreover, the spiral flatness decreases gradually with water depth, which is different from the first case.

The results of the third case are shown in Figure 1(g)–(i), where the vertical viscosity coefficient is $v_E(z) = 0.1 - 0.1e^{-\frac{\pi}{300}(h-z)}$, which equals to 0.07 $m^2\ s^{-1}$ at the sea surface and zero at the bottom. Compared with the second case, the vertical viscosity coefficient attenuates slowly in the water depth of 0–30 m and attenuates fast in the water depth below 60 m. In this case, $D_0 = 88.4$ m and $D = 86.0$ m. The surface current deflexion angle is 46.1° (Figure 1(h)). The flatness F_l is smaller than one (Figure 1(i)).

In the three cases of the vertical viscosity coefficients decreasing with water depth, the surface current deflexion angles are all larger than 45° although the magnitudes of angles are different. The surface liquid is under the effect of three forces: wind stress, friction force from underneath layer, and Coriolis force. When the three forces are in balance, the Ekman spiral is steady. For the case with constant vertical viscosity, the surface current deflexion angle is 45° and is on the right side of wind direction (for the Northern Hemisphere). Assuming the vertical viscosity coefficient changes from constant to decrease with water depth at a moment, the frictional resistance of underneath liquid on the surface liquid should decrease, which leads to the increasing surface current velocity, and the increasing Coriolis force. In this case, only if the surface current turns to the right, namely the surface current deflexion angle is larger than 45°, the new balance of three forces can be reached.

Price et al. (1986) observed that the deflexion angle is about 60° at the layer with depth of 2 m. The observation field is 400 km far away from San Diego, California, USA where the water depth is about 4000 m. During the observation period, the wind speed is about 3–12 m s^{-1}. Wind and surface waves lead to strong mixing in the upper ocean. So we can infer that the vertical viscosity coefficient is large at the sea surface during the observation time of Price et al. (1986) and decreases with water depth. It is similar to the vertical viscosity coefficients we have designed. With these vertical viscosity coefficients, the surface current deflexion angle is larger than 45°, which is consistent with the observation result of Price et al. (1986).

In all the three cases, the flatness F_l is smaller than one, but its changing trends are different because the three vertical viscosity coefficients have different attenuation speeds and attenuation forms. In the classical Ekman theory, the volume transport is about 0.671 and its direction is 90° to the right side of wind direction when wind stresses are set as the same as those in numerical calculation, i.e., $\tau^x = 0$ N m^{-2}, $\tau^y = 0.1$ N m^{-2}. From Table 1, one can see that the magnitude and direction of the volume transport we have computed in these three cases are almost the same as the results of classical Ekman theory. Namely, the magnitude and direction of volume transport of Ekman drift current are not influenced by the distributions of the attenuating vertical viscosity coefficients.

2.2 Vertical viscosity coefficient increasing and then decreasing with depth

In the Arctic and high latitude sea areas, the sea surface is covered by floating ice. So there is not enough long fetch for surface waves growing effectively. The turbulence generated by waves is very weak and the turbulence in the atmosphere cannot be transferred to the ocean through the sea ice. Below the sea surface, the existing internal waves and other physical processes can enhance the turbulence. Thus we can infer that the vertical viscosity coefficient is small at the sea surface, becomes larger below the sea surface, and then decreases with water depth in the Arctic and high latitude sea areas. In other words, the vertical viscosity coefficient increases first and then decreases with water depth. The behavior of the vertical viscosity coefficient can be idealized as

$$v_E(k) = 0.01 + 10^{-5} e^{z(k)}, \quad 0 \leqslant z \leqslant 9, \tag{7}$$

$$v_E(k) = 0.01 + 10^{-5} e^{z(kl)\left(1 - \frac{k+1-kl}{km+1-kl}\right)}, \quad 9 < z \leqslant 120, \tag{8}$$

where k is the layer number, $kl = 9$, $km = 61$, z is the water depth of different layers. The vertical viscosity coefficient reaches its largest value of 0.09 $m^2 s^{-1}$ at the water depth of 9 m (Figure 2(a)).

Figure 2(b) and 2(c) show the Ekman spiral structure and spiral flatness. The sea surface current deflexion angle is 32.4°, smaller than 45° (Figure 2(b)). This result is consistent with the observations in the Arctic and high latitude sea areas (Thorndike et al., 1982; Overland, 1994; Shu et al., 2012; Kimura et al., 2000; Fukamachi et al., 2011). In the near surface layer, the spiral flatness F_l is larger than one. And it decreases monotonously with water depth from surface to 9 m, and then increases gradually below water depth of 9 m.

With the given wind stress in this paper, the magnitude of the Ekman volume transport is 0.673 and its direction is 89.8° (Table 1). This result is identical with the magnitude and direction of volume transport of the classical Ekman theory. That is to say, the vertical viscosity coefficient which increases first and then decreases with depth can change the magnitude of the surface current deflexion angle and its spiral structure, but has no influence on the volume transport.

2.3 Vertical viscosity coefficient decreasing and then increasing

In the coastal area, turbulence is strong due to surface waves and other air-sea interface processes at the sea surface and is also strong due to tidal mixing at the sea bottom. So it can be inferred that the vertical viscosity coefficient decreases firstly and then increases with water depth in the coastal area and its idealized distribution can be given as

$$v_E(k) = 0.1 - 10^{-5} e^{z(k)}, \quad 0 \leqslant z \leqslant 9, \tag{9}$$

$$v_E(k) = 0.1 - 10^{-5} e^{z(kl)} \left(1 - \frac{k+1-kl}{km+1-kl}\right), \quad 9 < z \leqslant 120, \tag{10}$$

where k is the number of layers, $kl = 9$, $km = 61$, z is the water depth of different layers.

Figure 3 shows the distribution of the vertical viscosity coefficient and its corresponding Ekman spiral structure and spiral flatness. In this case, the vertical viscosity coefficient reaches its minimum value 0.02 $m^2 s^{-1}$ at water depth of 9 m. Its surface current deflexion angle is 54.8°, larger than 45°. The flatness is smaller than one at the sea surface layer. It is close to one in the depth from 9 to 60 m and then increases fast below the depth of 60 m. The magnitude of volume transport is about 0.676 and its direction is about 91.4°. This result is close to the result of the classical Ekman drift currents theory. In this case, $D_0 = 72.5$ m, $D = 82.4$ m, and both of them are smaller than the water depth we have chosen.

2.4 Vertical viscosity coefficient increasing with water depth

In the shallow sea area, when there are not wind and surface waves, the turbulence is strong at the sea bottom due to tidal mixing. The vertical viscosity coefficient should increase with water depth. In this case, we choose three kinds of vertical viscosity coefficients with different increasing styles and speeds (Figure 4, Table 1). They are exponential distri-

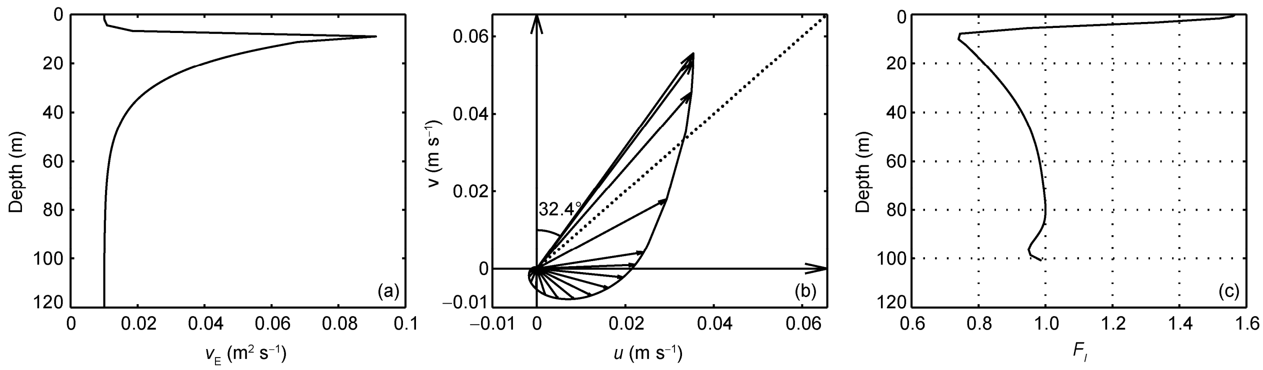

Figure 2 The vertical viscosity coefficient (a), the corresponding Ekman spiral structure (b) (with dot line indicating the 45° deflexion angle) and flatness F_l(c).

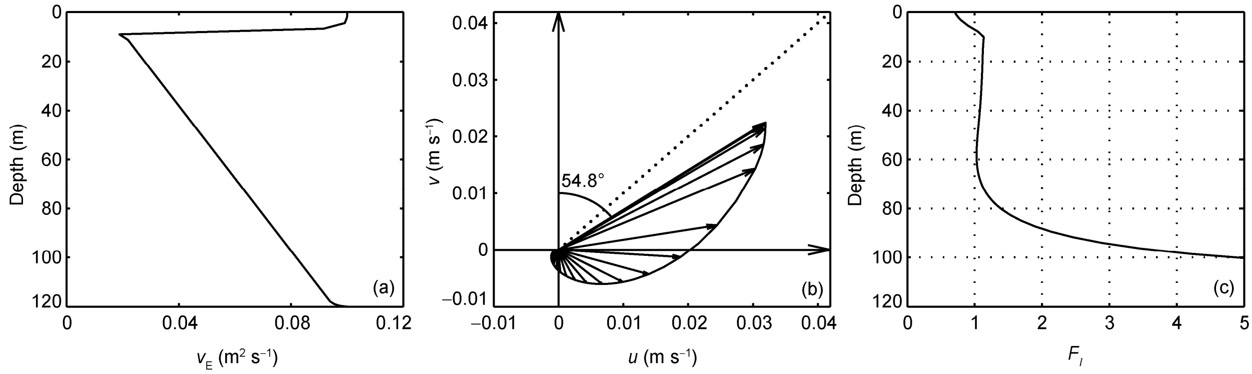

Figure 3 The vertical viscosity coefficient (a), the corresponding Ekman spiral structure (b) (with dot line indicating the 45° deflexion angle) and flatness F_l(c).

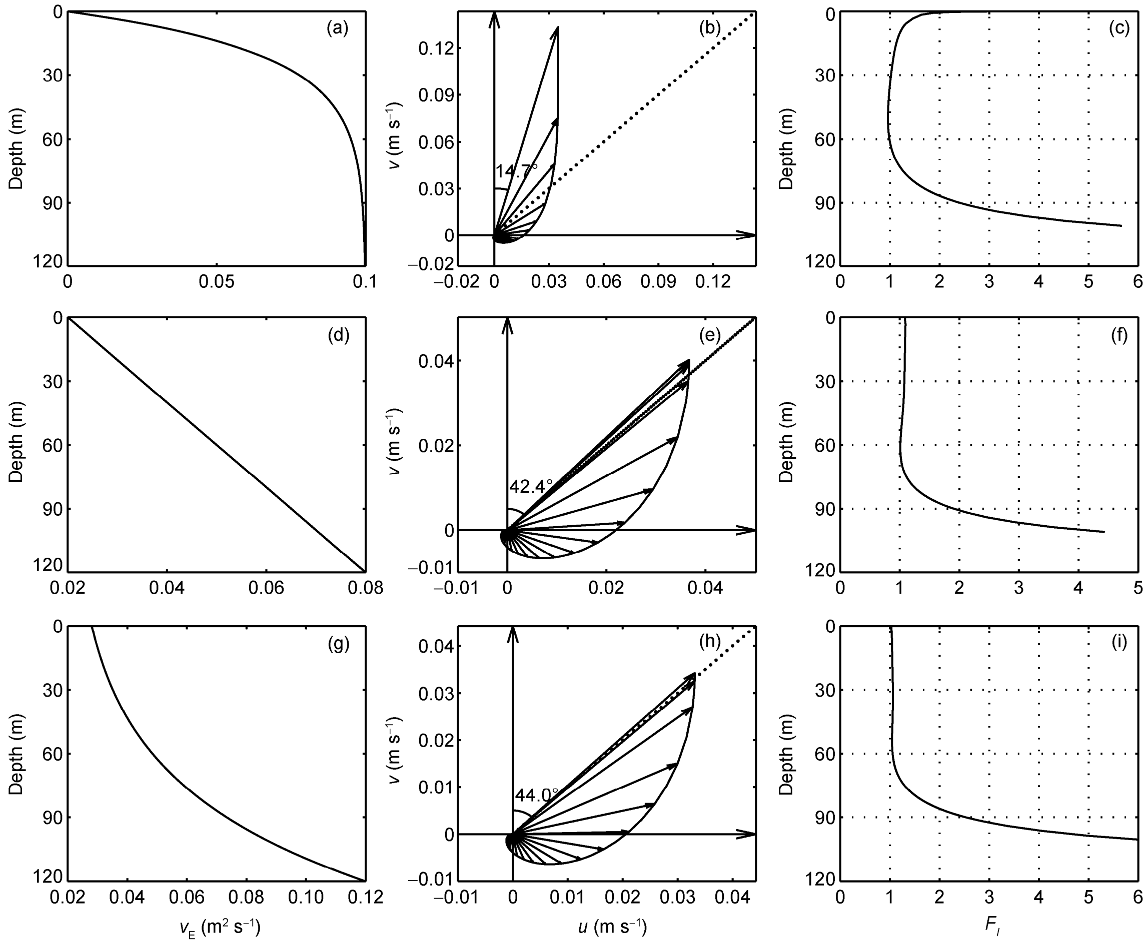

Figure 4 Three kinds of vertical viscosity coefficients ((a), (d) and (g)), and the corresponding Ekman spiral structures ((b), (e) and (h), with dot lines indicating the 45°deflexion angle) and flatness F_l ((c), (f) and (i)).

bution with fast increasing speed $v_E(z) = 0.100001 - 0.1\mathrm{e}^{-z/20}$, linear distribution $v_E(z) = 0.02 + 0.0005z$, and exponential distribution with slow increasing speed $v_E(z) = 0.02 + 0.1\mathrm{e}^{-\frac{\pi}{150}(h-z)}$.

Figures 4(a)–(c) show the results of the first case with the vertical viscosity coefficient of $v_E(z)$=$0.100001 - 0.1\mathrm{e}^{-z/20}$. The viscosity coefficient increases fast in the upper layer from 0 to 40 m. At the sea surface, it is 1×10^{-6} m^2 s^{-1} and increases to 0.08 m^2 s^{-1} at the water depth of 40 m. Below the depth of 40 m, the increase speed is slow. The Ekman depths, $D_0 = 47.6$ m, $D = 93.3$ m, are smaller than the water depth we have chosen so the obtained Ekman spiral is not influenced by the bottom boundary. Figure 4(b) shows that the surface current deflexion angle is about 14.7°, much smaller than 45°. The flatness is larger than one in the water depth from 0 to 20 m, namely, the speed of current velocity attenuation is larger than the speed of current direction turning. It is close to one from 20 to 60 m, and larger than one again in the water below 60 m.

For the second case, the vertical viscosity coefficient, $v_E(z)=0.02+0.0005z$, increases linearly, as shown in Figure 4(d). The Ekman depth, D_0=61.2 m, D=70.5 m. The surface current deflexion angle is about 42.4°, smaller than the result 45° of the classical Ekman theory. The flatness F_l is about one in the depth from 0 m to 60 m and is larger than one in the depth below 60 m.

For the third case, we choose the vertical viscosity coefficient as $v_E(z)=0.02+0.1\mathrm{e}^{-\frac{\pi}{150}(h-z)}$, which increases slowly in the depth from 0 to 60 m and increases fast below 60 m (Figure 4(g)). The Ekman depths, $D_0=65.7$ m, $D=72.6$ m, are smaller than the water depth we have set. The surface current deflexion angle is about 44.0°, slightly smaller than the value of the classical Ekman theory. The flatness F_l is about one from 0 to 60 m water depth and increases fast in the water depth below 60 m.

The numerical results suggest that when the vertical viscosity coefficients increase with water depth, the surface current deflexion angle is smaller than 45° although the magnitudes are different. Force analysis indicates that the surface liquid is under the effect of the three forces: wind stress, friction force from underneath layer, and Coriolis force. When the three forces are in balance, the Ekman drift current is steady. For the case with constant vertical viscosity, the surface current deflexion angel is 45° and is on the right side of wind direction (in the northern hemisphere). Assuming the vertical viscosity coefficient changes from constant to increase with water depth at a moment, the frictional resistance of underneath liquid on the surface liquid should increase, which leads to the decreasing surface current velocity, and the decreasing Coriolis force. In this case, only if the surface current turns to the left, namely, the surface current deflexion angle is smaller than 45°, the new balance of three forces can be reached.

The numerical results also show that the flatness is almost larger than one or equal to one at the sea surface and the bottom. That is to say, the speed of current attenuation equals to or is larger than the speed of current direction turning.

For all of the four categories of vertical viscosity coefficients, the magnitude and direction of volume transport are almost identical with the result of classical Ekman theory. Force analysis shows that the whole water column is under the effects of three forces, i.e., surface stress, Coriolis force, and friction force from sea bottom. However, the friction force can be ignored since the current velocity and its shear are very small at the bottom layer. So, when the two remaining forces are in balance, the direction of volume transport must be perpendicular to the wind direction and to the right side of wind (in the northern hemisphere). The magnitude of volume transport depends only on the wind stress and has no relationship with the distribution of vertical viscosity coefficient (Table 1).

3 Numerical simulation of the observed phenomenon

Price et al. (1986) observed that the surface current deflexion angle was about 60° in low-latitude ocean. The turbulence produced by surface waves should play an important role at the upper layer. We consider the wave-induced mixing proposed by Qiao et al. (2010)

$$Bv=\alpha A^3 k\omega \exp\{3kz\}, \tag{11}$$

where A is the wave amplitude, k is wave number, ω is frequency, and α is a coefficient, which is usually chosen as one. Price et al. (1986) showed that the north wind with 6.6 m s^{-1} at 10 m height was dominant during the observation. The wind stress is about –0.07 N m^{-2}, so we choose $\tau_y=0.07$ N m^{-2} in numerical simulation.

Meanwhile, given the wind speed at 10 m height, one can obtain the significant period T and significant wave height by using the following empirical formulas[1)]

$$T=0.75\times 0.91U_{10}, \tag{12}$$

$$H=0.22{U_{10}}^2/\mathrm{g}, \tag{13}$$

where U_{10} is the wind speed at 10 m height, g is the gravity acceleration. From the eqs. (12) and (13), one can get the significant period of 4.5 s and wave height of 0.98 m, and then we can calculate the vertical viscosity from eq. (11). Figure 5 shows the vertical viscosity coefficient, the corresponding spiral structure and flatness. One thing that we have to note is that the background vertical viscosity coefficient is chosen as 0.005 m^2 s^{-1} in this numerical simulation.

The maximum value of the vertical viscosity coefficient is about 0.07 m^2 s^{-1} at the surface and decreases very fast with depth. It reaches the minimum value 0.005 m^2 s^{-1} at 11 m water depth. The Ekman depths, $D_0=29.4$ m and $D=37.8$ m, are both smaller than the water depth we have set. The current is very small at the water depth of 80 m, so we just give the value of flatness F_l in the water depth from 0 to 80 m, as shown in Figure 5(c). Figure 5(b) tells us that

1) Stewart R H. 2008. Introduction to Physical Oceanography. Department of Oceanography Texas A&M University. 345.

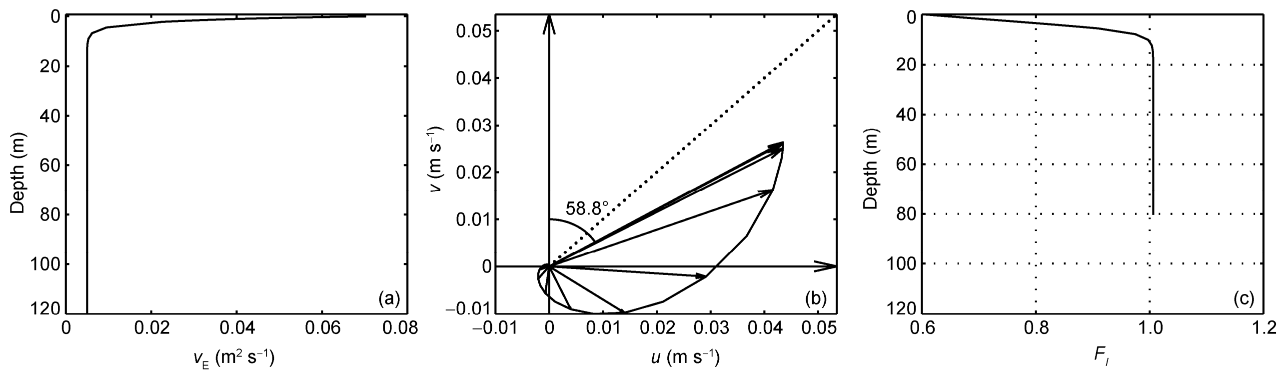

Figure 5 The vertical viscosity coefficient (a), the corresponding Ekman spiral structure (b) (with dot lines indicating the 45° deflexion angle), and flatness F_l (c).

the surface current deflexion angle is about 58.8°, which is very close to the observation of 60° (Price et al., 1986).

The vertical viscosity coefficient is only one physical factor that influences the current structure induced by wind. Other factors such as the non-homogenous or unsteady wind, and finite water depth, will also affect the structure of current induced by wind and the drifting direction of floating ice.

4 Discussions and conclusions

By assuming constant vertical viscosity, the classical Ekman theory shows that the deflexion angle is 45° and is on the right side of wind direction in the northern hemisphere and on the left side of wind direction in the southern hemisphere. But in the real ocean, the observations show that the surface current deflexion angle is smaller than 45° in the Arctic and high latitude oceans, larger than 45° in low latitude oceans.

In this paper, according to the physical processes occurring in different sea areas, the vertical viscosity coefficients are classified into four categories ideally and the influences of the different distributions of vertical viscosity coefficients on Ekman spiral structure are investigated with numerical methods. The numerical results show that the deflexion angle is larger than 45° when the vertical viscosity coefficient decreases with depth (corresponding to low and mid latitude oceans), which is identical with the observation of Price et al. (1986). The spiral flatness F_l is almost smaller than 1. When the vertical viscosity coefficient increases first and then decreases (corresponding to high latitude oceans or the Arctic), the deflexion angle is smaller than 45°, which is also identical with the observations in the Arctic and high latitude oceans. The flatness F_l can be larger or smaller than 1. When the vertical viscosity coefficient decreases first and then increases with depth (corresponding to coastal ocean with wind, surface waves, and tidal current), the deflexion angle is larger than 45°. The flatness F_l can also be larger or smaller than 1. When the vertical viscosity coefficient increases with depth (corresponding to coastal oceans with neither wind nor surface waves), the deflexion angle is smaller than 45°. The spiral flatness F_l is larger than 1. The numerical results also show that the volume transport of Ekman drift current is identical with the result of classical Ekman theory in deep water no matter what the distributions of vertical viscosity coefficients are. It is worth emphasizing that in this paper we aim to discuss the influence of different distribution characteristics of vertical viscosity coefficients on the Ekman spiral structure. Its basic assumptions are the same as those of the classical Ekman drift currents theory, namely, the homogeneous and steady wind acts on the infinitely broad sea surface for a long time. But in the real ocean, the factors, such as finite water depth, unsteady and non-homogenous wind and so on, will also have influence on the Ekman spiral structure. Consequently, the angle between the surface current direction and the wind direction does not equal 45°. Surface waves and other dynamical processes will have influence on the Ekman spiral structure and the volume transport (McWilliams et al., 1999; Polton et al., 2005; Huang, 1979). For instance, Huang (1979) had constructed the nonlinear theory framework to describe ocean drift movement by including the surface waves effect. He especially pointed out that the wind stress and sea surface wave states are the important factors that should be considered when studying the ocean drift current. It should be mentioned that the floating ice actually moves under the effect of the sea surface current and the current below the surface. So the deflexion angle of floating ice will be larger than that of surface current. But the observations indicate that the deflexion angle of floating ice is smaller than 45° in the Arctic.

In summary, the influence of vertical viscosity coefficients with different distribution characteristics on the Ekman spiral structure is investigated in this paper. It is found that the surface current deflexion angle is larger than 45° when the vertical viscosity coefficient in the upper ocean decreases with water depth, and smaller than 45° when it increases with water depth. Through analyzing the physical processes in different sea areas, we present a reasonable explanation to the observations that the surface current deflexion angle is smaller than 45° in the Arctic and high latitude oceans and the angle is larger than 45° in the low latitude oceans. Surface wave is an important physical process that happens at the air-sea interface. It can directly influence the strength of turbulence in the upper ocean, determine the distribution characteristic of vertical viscosity coefficient, and then influence the Ekman spiral structure and the surface current deflexion angle.

This work was supported by the National Natural Science Foundation of China (Grant No. 40876015), the Project of Comprehensive Evaluation of Polar Areas on Global and Regional Climate Changes (Grant No. CHINARE2012-04-04).

Ekman V W. 1905. On the influence of the earth's rotation on ocean-currents. Arkiv Math Astr Ocean Phys, 2: 1–51

Fukamachi Y, Ohshima K I, Mukai Y, et al. 2011. Sea-ice drift characteristics revealed by measurement of acoustic Doppler current profiler and ice-profiling sonar off Hokkaido in the Sea of Okhotsk. Ann Glaciol, 52: 1–8

Huang C J, Qiao F L, Dai D J, et al. 2012. Field measurement of upper ocean turbulence dissipation associated with wave-turbulence interaction in the South China Sea. J Geophys Res, 117: C00J09

Huang N E. 1979. On surface drift currents in the ocean. J Fluid Mech, 91: 191–208

Huang R X. 2009. Ocean Circulation: Wind-Driven and Thermohaline Processes. Cambridge: Cambridge University Press. 828

Jordan T F, Baker J R. 1980. Vertical structure of time-dependent flow dominated by friction in a well-mixed fluid. J Phys Oceanogr, 10: 1091–1103

Kimura N, Wakatsuchi M. 2000. Relationship between sea-ice motion and geostrophic wind in the northern hemisphere. Geophys Res Lett, 27: 3733–3738

Madsen O S. 1977. A realistic model of the wind-induced Ekman boundary layer. J Phys Oceanogr, 7: 248–255

McWilliams J C, Restrepo J M. 1999. The wave-driven ocean circulation. J Phys Oceanogr, 29: 2523–2540

Overland J E. 1994. Geostrophic drag coefficients for the central Arctic derived from Soviet station data. Tellus A, 46: 75–85

Polton J A, Lewis D M, Belcher S E. 2005. The role of wave-induced Coriolis-Stokes forcing on the wind-driven mixed layer. J Phys Oceanogr, 35: 444–457

Price J F, Sundermeyer M A. 1999. Stratified Ekman layers. J Geophys Res, 104: 20467–20494

Price J F, Weller R A, Pinkel R. 1986. Diurnal cycling: Observations and models of the upper ocean response to diurnal heating, cooling, and wind mixing. J Geophys Res, 91: 8411–8427

Price J F, Weller R A, Schudlich R R. 1987. Wind-driven ocean currents and Ekman transport. Science, 238: 1534–1538

Qiao F L, Yuan Y L, Ezer T, et al. 2010. A three-dimensional surface wave-ocean circulation coupled model and its initial testing. Ocean Dynam, 60: 1339–1355

Shu Q, Ma H Y, Qiao F L. 2012. Observation and simulation of a floe drift near the North Pole. Ocean Dynam, 62: 1195–1200

Thorndike A S, Colony R. 1982. Sea ice motion in response to geostrophic winds. J Geophys Res, 87: 5845–5852

Thomas J H. 1975. A theory of steady wind-driven currents in shallow water with variable eddy viscosity. J Phys Oceanogr, 5: 136–142

Ye A L, Li F Q. 1992. Physical Oceanography (in Chinese). Qingdao: Qingdao Ocean University Press. 384

Yuan Y L, Li H Q. 1993. Study on the structure and inducing mechanism of cold water mass of Yellow Sea-I. 0 order solution and circulation structure (in Chinese). Sci China Ser B, 23: 93–103